Organic Electronics 13 (2012) 1322–1328

Contents lists available at SciVerse ScienceDirect

Organic Electronics

journal homepage: www.elsevier.com/locate/orgel

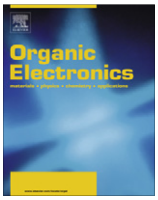

Synthesis of thieno[3,4-d]thiazole-based conjugated polymers and HOMO level tuning for high V_{OC} photovoltaic cell

Jea Woong Jo, Shin Sung Kim, Won Ho Jo *

WCU Hybrid Materials Program, Department of Materials Science and Engineering, Seoul National University, Seoul 151-742, Republic of Korea

ARTICLE INFO

Article history:
Received 27 February 2012
Received in revised form 3 April 2012
Accepted 6 April 2012
Available online 22 April 2012

Keywords:
Polymer solar cell
LUMO
Bulk heretojunction
Conjugated polymer

ABSTRACT

An electron-accepting building block, thieno[3,4-d]thiazole (TTz) was synthesized through a new synthetic route. When it was alternatively copolymerized with electron-donating fluorene, carbazole, or benzodithiophene derivatives *via* coupling reaction, all of the three copolymers had the low-lying lowest occupied molecular orbital energy levels around −3.55 eV, while the highest occupied molecular orbital (HOMO) energy level of the copolymer was dependent upon the electron-donating ability of electron-donating unit in the copolymer. When a fluorene derivative, the weakest electron-donating unit, was used as electron-donating building block, the copolymer showed the lowest HOMO energy. The alternating copolymer composed of TTz and fluorene derivative exhibits a high V_{OC} of 0.91 eV, because a weak electron-donating fluorene lowers the HOMO level of the alternating copolymer.

1. Introduction

Over the past decade, bulk heterojunction (BHJ) polymer solar cells have attracted much attention as low cost, flexible and printable energy devices [1–3]. Alternating copolymers with electron-donating and electron-accepting building blocks have been considered to be the most promising candidate for highly efficient polymer solar cells, because tunable energy levels of alternating copolymer may compensate a negative effect of [6,6]-phenyl-C_{61}-butyric acid methyl ester ($PC_{61}BM$) on the open circuit voltage (V_{OC}) due to its relatively low energy level of the lowest unoccupied molecular orbital (LUMO) (−4.0 to −4.3 eV) [4,5] and because the internal charge transfer between electron-donating and electron-accepting units in alternating copolymer can effectively reduce the bandgap and therefore extend the absorption range of the polymers [6,7]. In the recent years, remarkable progress has been achieved in this area, and as a result, the power conversion efficiencies (PCEs) over 7% have been obtained by using the weak electron-donating and strong electron-accepting building block strategy [8–11].

In developing new conjugated polymers for BHJ polymer solar cells, however, a few studies on electron-accepting building block in alternating polymer have been reported, while many studies have been focused on electron-donating building blocks such as benzo[1,2-b:4,5-b′]dithiophene [12], dithieno[3,2-b:2′,3′-d]silole [13], 2,7-carbazole [14], cyclopenta[2,1-b;3,4-b′]-dithiophene [15], and thiophene−phenylene−thiophene derivatives [16]. Although diketopyrrolopyrrole [17] and thieno[3,4-c]pyrrole-4,6-dione [18] with alkyl solubilizing group have recently been used as the electron-accepting building block for low bandgap donor polymers, the use of thieno-[3,4-b]thiophene (TT) is relatively unusual. The side alkyl chain of conjugated polymer is an important part of donor polymer in BHJ solar cells, because it controls aggregation of conjugated polymers [19,20], which is closely related to solubility, crystallinity, and morphology, and interaction at the interface between polymer and fullerene derivatives [21,22]. TT and its derivatives [4,12] have recently emerged as promising building blocks for synthesis of low-bandgap conjugated copolymers, because they can stabilize the quinoidal structure.

---

* Corresponding author. Tel.: +82 2 880 7192; fax: +82 2 876 6086.
E-mail address: whjpoly@snu.ac.kr (W.H. Jo).

1566-1199/$ - see front matter © 2012 Elsevier B.V. All rights reserved.
http://dx.doi.org/10.1016/j.orgel.2012.04.009

However, although TT units stabilize the quinoidal structure of the conjugated polymer, TT-based polymers have relatively high LUMO energy levels because of electron-rich characteristics of thiophene ring in TT. When $PC_{61}BM$ is used as an electron acceptor in BHJ solar cells, the energy levels of conjugated polymers should have the highest occupied molecular orbital (HOMO) energy levels between -5.2 and -5.7 eV and the LUMO energy levels between -3.5 and -3.9 eV for obtaining the optimum values of both V_{OC} and light harvesting [22]. Therefore, in this study, to lower the LUMO levels of TT and its derivatives, thieno[3,4-d]thiazole (TTz) monomer was synthesized and used as an electron-accepting building block of alternating conjugated copolymers. Although the chemical structure of TTz is similar to TT, TTz has more electron-deficient thiazole ring than thiophene. Therefore, it is expected that the thiazole ring in TTz not only stabilizes the quinoidal structure of the polymer backbone but also lowers the LUMO energy levels of alternating polymers.

2. Experimental

2.1. Materials

3-Amino-thiophene-2-carboxylic acid methyl ester (1) and nonanoyl chloride were purchased from Tokyo Chemical Industry and used without further purification. 2,7-Bis(4,4,5,5-tetramethyl-1,3,2-dioxaborolan-2-yl)-9-(tridecan-7-yl)-9*H*-carba-zole (6) [14] and 2,6-bis(trimethyltin)-4,8-bis(2-ethylhexyloxy)-benzo[1,2-b:4,5-b′]dithiophene (7) [11,24] were synthesized by following the methods reported in the literature. Tetrahydrofuran (THF) was dried over sodium/benzophenone under nitrogen and freshly distilled before use. Poly(3,4-ethylenedioxy-thiophene): poly(styrene sulfonate) (PEDOT:PSS) (Clevios P VP AI 4083) was purchased from H. C. Stark and passed through a 0.45 μm PVDF syringe filter before spin-coating. [6,6]-Phenyl-C_{71}-butyric acid methyl ester ($PC_{71}BM$) was obtained from Nano-C. All other reagents were purchased from Sigma–Aldrich and used as received.

2.2. Synthesis

2.2.1. 3-Amino-4-bromo-thiophene-2-carboxylic acid methyl ester (2)

Compound **1** (9 g, 57.3 mmol) was dissolved in acetic acid (80 mL) followed by dropwise addition of bromine (3.2 mL, 63 mmol) to the solution. After the reaction mixture was stirred at room temperature for 24 h, it was poured into saturated sodium thiosulfate solution and extracted with chloroform. The organic phase was collected and dried over $MgSO_4$. The product was purified by column chromatography on silica gel (1:20 ethyl acetate/hexane as eluent) to yield the compound **2** as a yellow solid (4.5 g, 33%). ^{1}H NMR (300 MHz, $CDCl_3$): δ (ppm) 7.29 (s, 1H), 5.63 (s, 2H), 3.84 (s, 3H). ^{13}C NMR (125 MHz, $CDCl_3$): δ (ppm) 164.25, 150.57, 128.24, 102.63, 100.61, 51.72. *m*/*z* (MS-EI) calcd: 234.9, found: 235.4.

2.2.2. Nonanoic acid (4-bromo-thiophen-3-yl)-amide (3)

To a solution of compound **2** (1 g, 4.25 mmol) in methanol (40 mL), water (7 mL) and NaOH (1 g) were added, and the mixture was refluxed for 1.5 h. The solution was then cooled to room temperature before conc. HCl (8 mL) was added dropwise. After stirring at 40 °C for 1.5 h, the solution was diluted with water and neutralized with $NaHCO_3$ (6 g). The solution was extracted with ethyl acetate, washed with water, and dried over $MgSO_4$. The solution was concentrated under reduced pressure, and the concentrated solution was dissolved in methylene chloride (15 mL) in the presence of triethylamine (TEA) (1.2 mL, 8.5 mmol). After the solution mixture was cooled by an ice-water bath, nonanoyl chloride (1.2 mL, 6.38 mmol) was added dropwise. After stirring overnight at ambient temperature, the reaction mixture was poured into water and extracted with methylene chloride. The organic phase was dried over $MgSO_4$, and the solvent was evaporated under reduced pressure. The crude product was purified by column chromatography on silica gel (1:5 ethyl acetate/hexane as eluent) to afford compound **3** as a white solid (670 mg, 50%). ^{1}H NMR (300 MHz, $CDCl_3$): δ (ppm) 7.90 (d, 1H), 7.52 (s, 1H), 7.22 (d, 1H), 2.41 (t, 2H), 1.74 (m, 2H), 1.28 (m, 10H), 0.88 (t, 3H). ^{13}C NMR (125 MHz, $CDCl_3$): δ (ppm) 170.77, 132.76, 121.46, 110.57, 103.25, 37.43, 32.02, 29.51, 29.42, 29.33, 25.72, 22.85, 14.29. *m*/*z* (MS-EI) calcd: 317.0, found: 317.5.

2.2.3. Nonanethioic acid (4-bromo-thiophen-3-yl)-amide (4)

The compound **3** (3.4 g, 10.7 mmol) and Lawesson's reagent (2.4 g, 5.89 mmol) were dissolved in 30 mL of THF. The reactant was refluxed overnight, and then silica gel was added. After evaporating the solvent, the product was purified by column chromatography on silica gel (1:4 chloroform/hexane as eluent) to afford viscous yellow oil as product (3.57 g, 82%). ^{1}H NMR (300 MHz, $CDCl_3$): δ (ppm) 9.03 (d, 1H), 8.99 (s, 1H), 7.30 (d, 1H), 2.87 (t, 2H), 1.87 (m, 2H), 1.28 (m, 10H), 0.88 (t, 3H). ^{13}C NMR (125 MHz, $CDCl_3$): δ (ppm), 202.61, 133.68, 121.60, 114.24, 104.97, 49.45, 31.97, 29.70, 29.46, 29.29, 28.98, 22.80, 14.26. *m*/*z* (MS-EI) calcd: 333.0, found: 333.3.

2.2.4. 2-Octyl-thieno[3,4-d]thiazole (TTz)

To a solution of compound **4** (800 mg, 2.39 mmol) in *N*-methyl-2-pyrrolidone (NMP) (10 mL) was added NaH (60% dispersion in mineral oil, 115 mg, 2.87 mmol) and the resulting reaction mixture was heated to 140 °C for 24 h. Then, it was poured into 1 M $NaHCO_3$ solution and extracted with chloroform. After organic extracts were dried over $MgSO_4$ and filtered, the solvent was evaporated under reduced pressure. The crude product was purified by column chromatography on silica gel (1:5 chloroform/hexane as eluent) to yield the compound TTz as a yellow oil (275 mg, 45%). ^{1}H NMR (300 MHz, $CDCl_3$): δ (ppm) 7.45 (d, 1H), 7.16 (d, 1H), 2.98 (t, 2H), 1.84 (m, 2H), 1.27 (m, 8H), 0.88 (t, 3H). ^{13}C NMR (125 MHz, $CDCl_3$): δ (ppm) 179.07, 160.19, 134.36, 109.91, 109.57, 35.56, 32.01, 29.45, 29.33, 29.32, 29.10, 22.84, 14.28. *m*/*z* (MS-EI) calcd: 253.1, found: 253.2.

2.2.5. 4,6-Dibromo-2-octyl-thieno[3,4-d]thiazole (TTz-Br)

The compound TTz (275 mg, 1.09 mmol) was dissolved in 5 ml of THF, to which *N*-bromosuccinimide (NBS) (400 mg, 2.25 mmol) was added in the dark. After stirring the mixture overnight at room temperature, the solvent was removed under reduced pressure, and then the product was purified by column chromatography on silica (1:20 ethyl acetate/hexane as eluent) to afford TTz-Br as an orange oil (390 mg, 87%). ^{1}H NMR (300 MHz, $CDCl_3$): δ (ppm) 2.97 (t, 2H), 1.81 (m, 2H), 1.28 (m, 8H), 0.88 (t, 3H). ^{13}C NMR (125 MHz, $CDCl_3$): δ (ppm) 180.59, 156.94, 135.91, 95.58, 95.44, 35.84, 31.99, 29.40, 29.32, 29.28, 29.24, 22.84, 14.29. *m*/*z* (MS-EI) calcd: 411.2, found: 411.4.

2.2.6. Polymer PFTTz

Monomer **5** (157 mg, 0.37 mmol) and TTz-Br (153 mg, 0.37 mmol) was dissolved in a mixture of THF (16 mL) and aqueous K_2CO_3 solution (2 M, 4 mL). After the solution was flushed with N_2 for 20 min, 20 mg of $Pd(PPh_3)_4$ was added. The reaction mixture was stirred at 70 °C for 48 h. After being cooled to room temperature, the mixture was poured into methanol. The crude product was filtered through a Soxhlet thimble, and then subjected to Soxhlet extraction with methanol, ethyl acetate, hexane, acetone, and chloroform. The polymer was recovered from the chloroform fraction, and precipitated into methanol to afford the product as an orange solid (100 mg, 46%). ^{1}H NMR (300 MHz, $CDCl_3$): δ (ppm) 8.40–8.10 (m, 2H), 7.80 (d, 2H), 7.68 (d, 2H), 3.14 (t, 2H), 2.30–0.80 (br, 41H).

2.2.7. Polymer PCTTz

PCTTz was synthesized by following the same procedure as used in the synthesis of PFTTz. Monomer **6** (232 mg, 0.39 mmol) and TTz-Br (159 mg, 0.39 mmol) were used as monomers, and an orange solid was obtained as a product (149 mg, 64%). ^{1}H NMR (300 MHz, $CDCl_3$): δ (ppm) 8.40–6.90 (br, 6H), 4.90–4.40 (br, 1H), 3.30–2.80 (br, 2H), 2.50–0.80 (br, 41H).

2.2.8. Polymer PBTTz

Monomer **7** (160 mg, 0.21 mmol) and TTz-Br (85 mg, 0.21 mmol) was dissolved in toluene. After the solution was flushed with N_2 for 20 min, and then 20 mg of $Pd(PPh_3)_4$ was added. The reaction mixture was stirred at 110 °C for 48 h. After being cooled to room temperature, the resulting mixture was poured into methanol. The crude product was filtered through a Soxhlet thimble, and then subjected to Soxhlet extraction with methanol, ethyl acetate, hexane, acetone, and chloroform. The polymer was recovered from the chloroform fraction, and precipitated into methanol to afford the product as a blue solid (117 mg, 80%). ^{1}H NMR (300 MHz, $CDCl_3$): δ (ppm) 7.90–6.90 (br, 2H), 4.50–3.80 (br, 4H), 3.30–2.80 (br, 2H), 2.40–0.80 (br, 45H).

2.3. Characterization

The chemical structures of compounds were identified by ^{1}H NMR (Avance DPX-300) and ^{13}C NMR (Avance DPX-500). Molar masses of compounds were measured on a Jeol JMS600w in electron-impact mode. Molecular weight and distribution of polymers were measured by GPC (Waters) with a refractive index detector (Waters 2414). THF was used as an eluent, and the molecular weight of polymers were calibrated by polystyrene standards. The optical absorption spectra were obtained by a UV–Vis spectrophotometer (Lambda 25, Perkin Elmer). Cyclic voltammetry were conducted on a potentiostat/galvanostat (VMP 3, Biologic) in an electrolyte solution of 0.1 M tetrabutylammonium hexafluorophosphate in dichloromethane. Pt wires (Bioanalytical System Inc.) were used as both counter and working electrodes, and silver/silver ion (Ag in 0.1 M $AgNO_3$

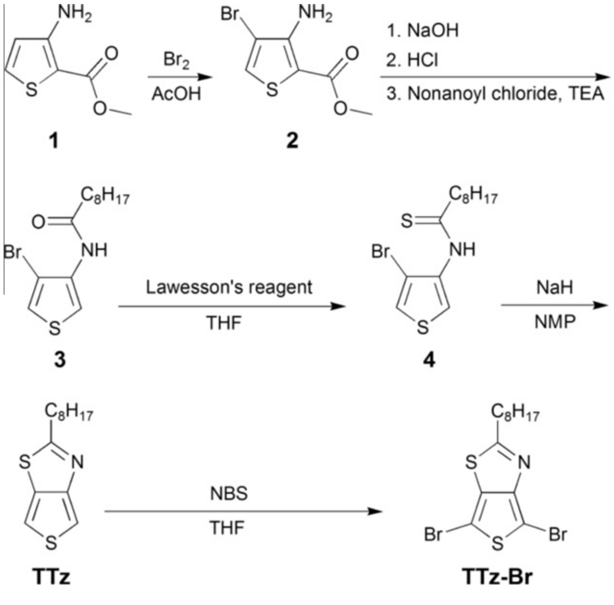

Scheme 1. Synthesis of TTz and TTz-Br.

solution, Bioanalytical System Inc.) was used as a reference electrode. The HOMO energy levels of polymers were calculated by using the equation: HOMO (V) = $-[E_{ox} - E_{1/2}$(ferrocene) + 4.8], where E_{ox} is the onset oxidation potential of the polymer and $E_{1/2}$(ferrocene) is the onset oxidation potential of ferrocene vs. Ag/Ag$^+$. The LUMO energy levels were also estimated by using the equation: LUMO (V) =$-[E_{red} - E_{1/2}$(ferrocene) + 4.8], where E_{red} is the onset reduction potential of the polymer.

2.4. Device fabrication and characterization

The polymer solar cells were fabricated with a standard device configuration of glass/ITO/PEDOT:PSS/polymer: $PC_{71}BM$/Al. To fabricate polymer solar cells, ITO-coated glass was first cleaned with acetone and isopropyl alcohol. After complete drying, the ITO-coated glass was treated with UV-ozone for 15 min. PEDOT:PSS was spin-coated with 40 nm thickness on the ITO-coated glass and annealed at 120 °C for 30 min. A 2 wt.% blend solution of polymer/$PC_{71}BM$ are dissolved in chlorobenzene (PBTTz/$PC_{71}BM$ dissolved in *o*-dichloro-benzene), and spin-coated on the top of the PEDOT:PSS layer at 800–1200 rpm for 40 s. The film thickness of the active layer was measured by surface profiler (AlphaStep IQ, KLA Tencor). The active layer thicknesses in the devices of PFTTz, PCTTz and PBTTz were 90, 80 and 120 nm, respectively. Aluminum (100 nm) was thermally evaporated on the top of the active layer under vacuum ($<10^{-6}$ Torr). The effective area of the cell was ca. 4 mm^2. The current density–voltage (*J*–*V*) characteristics were measured with a Keithley 4200 source-meter under AM 1.5G (100 mW/cm^2) simulated by a Newport-Oriel solar simulator. The light intensity was calibrated using a NREL-certified photodiode prior to each measurement. The external quantum efficiency (EQE) was measured using a Polaronix K3100 IPCE measurement system (McScience). The light intensity at each wavelength was calibrated with a standard single-crystal Si cell. The morphologies of polymer/$PC_{71}BM$ blend films were observed by a transmission electron microscope (TEM) (JEOL, JEM-1010).

3. Results and discussion

3.1. Synthesis and characterization

The synthetic route for monomers and polymers were illustrated in Scheme 1 and Scheme 2, respectively. In previous report [25], TTz was synthesized by cyclization of thiophene ring from thiazole derivatives, but the method is very complicated with many synthetic steps. Hence, we have developed a more effective synthetic pathway for synthesis of TTz starting from commercially available thiophene derivative **1**. First, bromination of **1** with bromine in acetic acid solution produces the compound **2** with

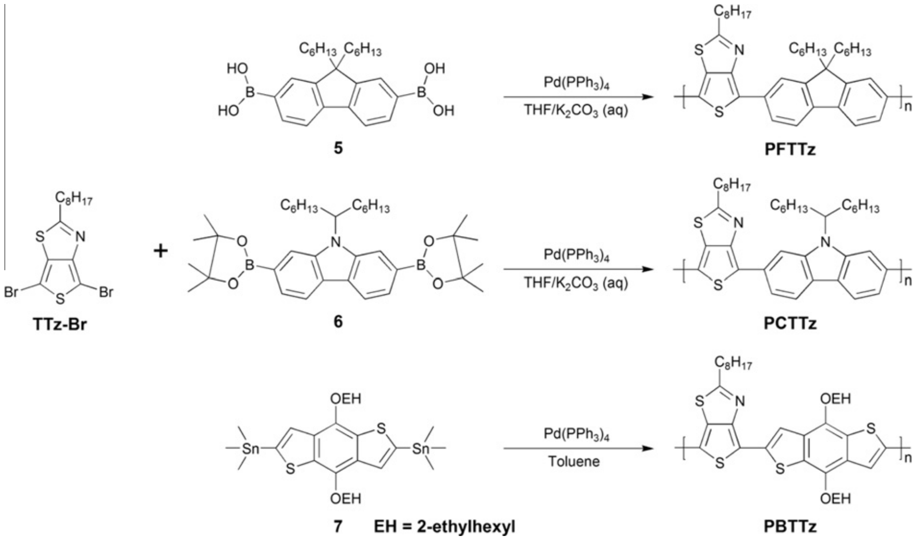

Scheme 2. Synthesis of TTz-based copolymers.

Table 1
Characteristics of TTz-based polymers.

Polymer	M_n (kg/mol)	PDI	UV–Vis absorption		$E_g$opt[a] (eV)	HOMO (eV)	LUMO (eV)	$E_g$ec[b] (eV)
			λ_{max} ($CHCl_3$) (nm)	λ_{max} (film) (nm)				
PFTTz	36	2.6	484, 507	491, 519	2.17	−5.58	−3.55	2.03
PCTTz	43	2.6	495, 525	497, 527	2.11	−5.46	−3.56	1.90
PBTTz	10	1.2	581, 627	583, 634	1.73	−5.24	−3.57	1.67

[a] Determined from the onset of UV–Vis absorption spectra.
[b] Determined from the cyclic voltammetry.

a moderate yield (33%). After saponification and decarboxylation of ester group on 2-position of thiophene, the compound **3** was obtained with 50% yield by reacting amine on thiophene in **2** with nonanoyl chloride in the presence of TEA. The amide group on **3** was then converted to thioamide group using the Lawesson's reagent in THF. Ring cyclization of compound **4** with NaH results in TTz with 45% yield. Finally, TTz is easily brominated with NBS to afford TTz-Br monomer for polymerization.

Polymers PFTTz, PCTTz and PBTTz were synthesized *via* the Suzuki or Stille coupling reactions using $Pd(PPh_3)_4$ as a catalyst. All synthesized polymers are highly soluble in common organic solvents such as chloroform, chlorobenzene, and dichlorobenzene at room temperature. It should be noted that the molecular weight of polymers and its polydispersity index (PDI) are measured by GPC and listed in Table 1.

3.2. Optical properties

The UV–Vis absorption spectra of polymers in chloroform solution and film state are shown in Fig. 1, and these spectroscopic data are summarized in Table 1. The red shift in film state compared to the absorption maximum of chloroform solution indicates an increased π–π stacking of polymer backbone in solid film. When the optical bandgaps of polymers are calculated from the absorption

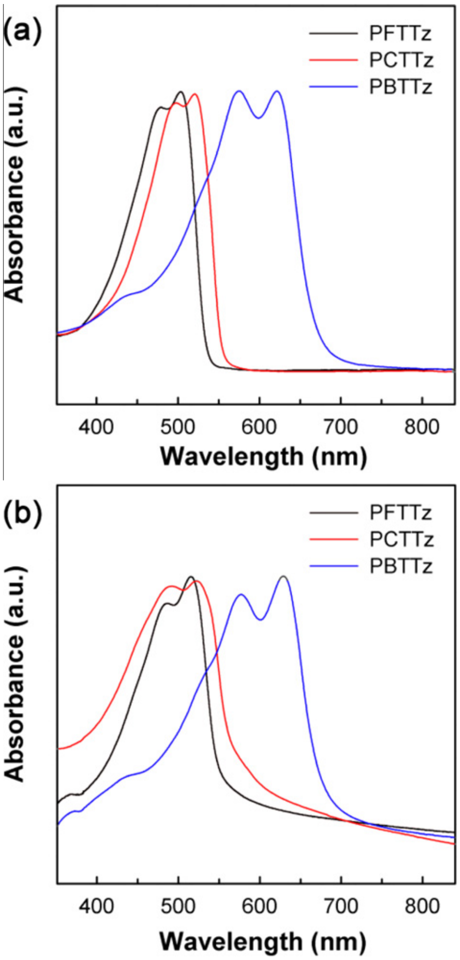

Fig. 1. UV–Vis absorption spectra of polymers in chloroform solution (a) and in film state (b).

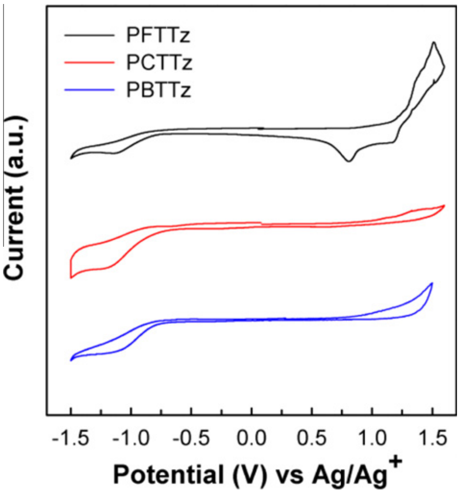

Fig. 2. Cyclic voltammograms of polymers.

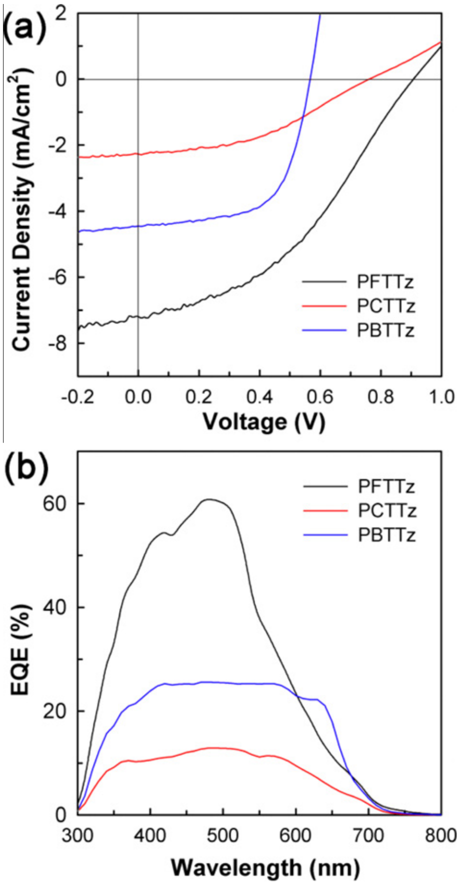

Fig. 3. *J–V* curves of polymer/$PC_{71}BM$ BHJ solar cells under AM 1.5G, 100 mW/cm^2 (a), and EQE spectra of solar cells (b).

Table 2
Photovoltaic properties of devices under standard AM 1.5G illumination.

Polymer	Polymer:$PC_{71}BM$ (w/w)	V_{OC} (V)	J_{SC} (mA/cm^2)	FF	PCE (%)
PFTTz	1:2	0.91	7.20	0.40	2.64
PCTTz	1:2	0.76	2.27	0.41	0.71
PBTTz	1:3	0.52	4.64	0.58	1.41

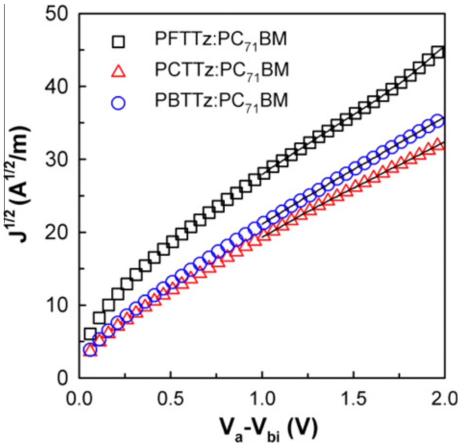

Fig. 4. Dark *J–V* characteristics of PFTTz:$PC_{71}BM$ (1:2 w/w), PCTTz:$PC_{71}BM$ (1:2 w/w) and PBTTz:$PC_{71}BM$ (1:3 w/w) blends with hole-only device. The solid lines are the best linear fit of the data point.

edge of thin film, the bandgaps of PFTTz, PCTTz and PBTTz are 2.17, 2.11 and 1.73 eV, respectively. In donor–acceptor type alternating polymer, the LUMO energy level of polymer is dominantly affected by electron-accepting building block, while the HOMO energy level is controlled by electron-donating unit. Since three polymers synthesized in this study have identical electron-accepting unit, it is expected that the LUMO levels of the copolymers are nearly the same while the HOMO levels are dependent upon the electron-donating ability of electron-donor unit in the copolymer, and as a result the bandgaps of the alternating copolymers are governed by electron-donating units. Since the electron-donating ability is in the order of benzodithiophene, carbazole and fluorene, the bandgaps of the polymers become lower in the order of PBTTz, PCTTz and PFTTz, as can be seen in Table 1.

3.3. Electrochemical properties

The electrochemical properties of the polymers were measured from oxidation and reduction cyclic voltammetry (Fig. 2), and the data are listed in Table 1. The electrochemically measured bandgaps ($E_g$ec) of polymers are well consistent with the optical bandgap ($E_g$opt) determined from UV–Vis absorption spectra. The LUMO energy levels of all the polymers are around −3.55 eV, which is lower than those of commonly used TT derivatives (−3.20 to −3.45 eV) [4,12] and located in ideal LUMO energy level range (−3.5 to −3.9 eV) for high efficient solar cells [23]. Furthermore, the LUMO energy offsets between our copolymers and PCBM (−4.0 eV) are sufficient for exciton dissociation at the interface between polymers and PCBM [26].

Since electron-richer environment induced by thiophene in benzodithiophene leads to higher HOMO energy level (−5.24 eV) of PBTTz than the other copolymers, PBTTz may exhibit the lowest V_{OC}, because V_{OC} is proportional to the difference the HOMO energy level of donor polymer and the LUMO energy level of acceptor (PCBM).

3.4. Photovoltaic properties

The current density–voltage (*J–V*) curves are shown Fig. 3a, from which photovoltaic parameters are evaluated (Table 2). Since deeper HOMO energy level of donor polymer yields higher V_{OC}, the V_{OC} of PFTTz (0.91 V) is higher than other two polymers, PCTTz and PBTTz. To this end, PFTTz exhibits higher PCE of 2.64% than others.

The J_{sc} values caculated from the integration of EQE spectra (Fig. 3b) agree well with the J_{sc} values from *J–V* curves. Although PFTTz shows limited absorption below 550 nm while PBTTz exhibits strong absorption up to 700 nm, as shown in Fig. 1a, PFTTz has larger EQE value than PCTTz and PBTTz, showing considerably high EQE of 61% at 480 nm.

To investigate the mismatch between absorption and EQE, hole mobilities were measured from dark *J–V* curve by using the space charge limited current model (Fig. 4). When the hole mobilities of PFTTz/$PC_{71}BM$, PCTTz/$PC_{71}BM$, and PBTTz/$PC_{71}BM$ are compared, the hole mobility of PBTTz/$PC_{71}BM$ (1.1×10^{-4} cm^2 V^{-1} s) is still higher than those of PFTTz/$PC_{71}BM$ (4.8×10^{-5} cm^2 V^{-1} s) and PCTTz/$PC_{71}BM$ (4.0×10^{-5} cm^2 V^{-1} s). When the morphologies of polymer/$PC_{71}BM$ blend films are examined by TEM, as shown in Fig. 5, it revealed that the PFTTz/$PC_{71}BM$ film exhibits well-developed nanoscale phase-separated

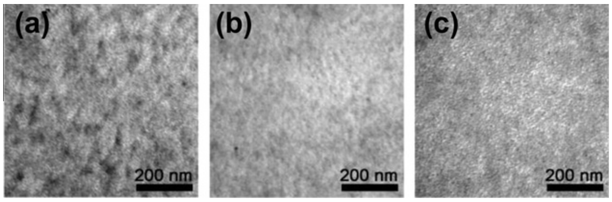

Fig. 5. TEM images of polymer/$PC_{71}BM$ blend films PFTTz:$PC_{71}BM$ (1:2 w/w) (a), PCTTz:$PC_{71}BM$ (1:2 w/w) (b) and PBTTz:$PC_{71}BM$ (1:3 w/w) (c).

morphology, whereas the PCTTz/$PC_{71}BM$ and PBTTz/$PC_{71}BM$ films show homogeneously mixed morphology. Since nanoscale phase-separated morphology with interconnected network structure is essential for effective exciton dissociation and charge transport [27], PBTTz does not show higher EQE and J_{SC} than PFTTz, although PBTTz exhibits stronger absorption and higher hole mobility than PFTTz.

4. Conclusions

We have successfully synthesized TTz by a new and effective synthetic method and TTz-based alternating copolymers by coupling reaction. While the copolymers showed the relatively low-lying LUMO energy levels of around −3.55 eV due to electron-withdrawing thiazole ring in TTz, the HOMO energy levels and the bandgaps of the copolymers were dependent upon the electron-donating ability of electron-donor unit in the copolymers. A PCE of 2.64% with a high V_{oc} of 0.91 V were achieved from PFTTz/$PC_{71}BM$ blend under AM 1.5G illumination (100 mW/cm^2). Since higher PCE is expected by a further precise device optimization, TTz is a promising electron-accepting building block in donor–acceptor type alternating copolymer to achieve high performance solar cells.

Acknowledgment

The authors thank the Ministry of Education, Science and Technology, Korea for financial support through the Global Research Laboratory (GRL) and the World Class University (WCU) programs.

References

[1] N.S. Sariciftci, L. Smilowitz, A.J. Heeger, F. Wudl, Science 258 (1992) 1474.
[2] G. Yu, J. Gao, J.C. Hummelen, F. Wudl, A.J. Heeger, Science 270 (1995) 1789.
[3] J.W. Jung, W.H. Jo, Adv. Funct. Mater. 20 (2010) 2355.
[4] H.Y. Chen, J.H. Hou, S.Q. Zhang, Y.Y. Liang, G.W. Yang, Y. Yang, L.P. Yu, Y. Wu, G. Li, Nat. Photonics 3 (2009) 649.
[5] H.X. Zhou, L.Q. Yang, A.C. Stuart, S.C. Price, S.B. Liu, W. You, Angew. Chem. Int. Ed. 50 (2011) 2995.
[6] Y. Lee, Y.M. Nam, W.H. Jo, J. Mater. Chem. 21 (2011) 8583.
[7] N. Blouin, A. Michaud, D. Gendron, S. Wakim, E. Blair, R. Neagu-Plesu, M. Belletete, G. Durocher, Y. Tao, M. Leclerc, J. Am. Chem. Soc. 130 (2008) 732.
[8] H.X. Zhou, L.Q. Yang, S.C. Price, K.J. Knight, W. You, Angew. Chem. Int. Ed. 49 (2010) 7992.
[9] T.Y. Chu, J.P. Lu, S. Beaupre, Y.G. Zhang, J.R. Pouliot, S. Wakim, J.Y. Zhou, M. Leclerc, Z. Li, J.F. Ding, Y. Tao, J. Am. Chem. Soc. 133 (2011) 4250.
[10] S.C. Price, A.C. Stuart, L.Q. Yang, H.X. Zhou, W. You, J. Am. Chem. Soc. 133 (2011) 4625.
[11] C.E. Small, S. Chen, J. Subbiah, C.M. Amb, S. Tsang, T. Lai, J.R. Reynolds, F. So, Nat. Photonics 6 (2012) 115.
[12] Y.Y. Liang, D.Q. Feng, Y. Wu, S.T. Tsai, G. Li, C. Ray, L.P. Yu, J. Am. Chem. Soc. 131 (2009) 7792.
[13] J.H. Hou, H.Y. Chen, S.Q. Zhang, G. Li, Y. Yang, J. Am. Chem. Soc. 130 (2008) 16144.
[14] N. Blouin, A. Michaud, M. Leclerc, Adv. Mater. 19 (2007) 2295.
[15] D. Muhlbacher, M. Scharber, M. Morana, Z.G. Zhu, D. Waller, R. Gaudiana, C. Brabec, Adv. Mater. 18 (2006) 2884.
[16] S.H. Chan, C.P. Chen, T.C. Chao, C. Ting, C.S. Lin, B.T. Ko, Macromolecules 41 (2008) 5519.
[17] M.M. Wienk, M. Turbiez, J. Gilot, R.A.J. Janssen, Adv. Mater. 20 (2008) 2556.
[18] Y.P. Zou, A. Najari, P. Berrouard, S. Beaupre, B.R. Aich, Y. Tao, M. Leclerc, J. Am. Chem. Soc. 132 (2010) 5330.
[19] L.Q. Yang, H.X. Zhou, W. You, J. Phys. Chem. C 114 (2010) 16793.
[20] C. Piliego, T.W. Holcombe, J.D. Douglas, C.H. Woo, P.M. Beaujuge, J.M.J. Frechet, J. Am. Chem. Soc. 132 (2010) 7595.
[21] J.M. Szarko, J.C. Guo, Y.Y. Liang, B. Lee, B.S. Rolczynski, J. Strzalka, T. Xu, S. Loser, T.J. Marks, L.P. Yu, L.X. Chen, Adv. Mater. 22 (2010) 5468.
[22] Z. Li, Y.G. Zhang, S.W. Tsang, X.M. Du, J.Y. Zhou, Y. Tao, J.F. Ding, J. Phys. Chem. C 115 (2011) 18002.
[23] G. Dennler, M.C. Scharber, C.J. Brabec, Adv. Mater. 21 (2009) 1323.
[24] J.H. Hou, M.H. Park, S.Q. Zhang, Y. Yao, L.M. Chen, J.H. Li, Y. Yang, Macromolecules 41 (2008) 6012.
[25] I.T. Kim, J.H. Lee, S.W. Lee, Bull. Korean Chem. Soc. 28 (2007) 2511.
[26] D. Veldman, S.C.J. Meskers, R.A.J. Janssen, Adv. Funct. Mater. 19 (2009) 1939.
[27] M.A. Ruderer, S. Guo, R. Meier, H. Chiang, V. Körstgens, J. Wiedersich, J. Perlich, S.V. Roth, P. Müller-Buschbaum, Adv. Funct. Mater. 21 (2011) 3382.